

Original Research

The Influence of Plasma Nitriding Process Conditions on the Microstructure of Coatings Obtained on the Substrate of Selected Tool Steels

Magdalena Mokrzycka¹ , Adrianna Przybyło² , Marek Góral^{1,*} , Barbara Kościelniak¹ , Marcin Drajewicz¹ , Tadeusz Kubaszek¹ , Kamil Gancarczyk¹ , Andrzej Gradzik¹ , Kamil Dychtoń¹ , Marek Poręba¹ , Jakub Jopek¹ , Maciej Pytel¹ 

¹ Rzeszow University of Technology, Research and Development Laboratory for Aerospace Materials, Zwirki i Wigury 4, 35-959 Rzeszow, Poland; magdamok007@wp.pl (M. Mokrzycka), b.koscielnia@prz.edu.pl (B. Kościelniak), drajewicz@prz.edu.pl (M. Drajewicz), tkubaszek@prz.edu.pl (T. Kubaszek), Kamil-Gancarczyk@prz.edu.pl (K. Gancarczyk), andrzej_gradzik@prz.edu.pl (A. Gradzik), kdychton@prz.edu.pl (K. Dychtoń), poreba@prz.edu.pl (M. Poręba), jakub.jopek01@gmail.com (J. Jopek), mpytel@prz.edu.pl (M. Pytel)

² Doctoral School of Engineering and Technical Sciences at the Rzeszow University of Technology, Rzeszow University of Technology, Powstancow Warszawy 12, Rzeszow, 35-959, Poland; przybylo.ada@gmail.com

* Correspondence: mgoral@prz.edu.pl

Received: 28 March 2023 / Accepted: 19 September 2023 / Published online: 5 January 2024

Abstract

This study presents the results of research into the influence of the time of the plasma nitriding process on the microstructure of the coatings obtained. Cold-work tool steels (60WCrV8, 90MnCrV8, 145Cr6), hot-work tool steel (X37CrMoV5-1) and high-speed tool steel (HS6-5-2) were selected as substrate material. The processes were carried out under industrial conditions using an Ionit device from Oerlikon Metaplas with variable process times of 2, 4 and 6 hours. According to literature data, a nitriding mixture consisting of 5% nitrogen and 95% hydrogen was chosen, which allowed the expected diffusion layer to be obtained without a white layer (composed of iron nitrides). Analysis of elemental mapping indicates that the presence and content of nitride-forming elements influences the formation of alloy additive nitrides in the microstructure of the diffusion layer. It was also found that an increase in the duration of plasma nitriding, results in an increase in the depth of the nitrided layers formed on the substrate of high-alloy steels: X37CrMoV5-1 and HS6-5-2. Nitrides of alloying additives, present in the diffusion layer, are formed in the high-alloyed the hot-work steel X37CrMoV5-1, indicating that these steels are the most suitable for plasma nitriding of the entire tool steels analysed.

Keywords: plasma nitriding, tool steel, heat treatment, kinetic of nitriding

1. Introduction

Thermochemical treatment processes are performed to improve tribological and mechanical properties and increase corrosion resistance. They are implemented by combining thermal treatments with a targeted change in the chemical composition of the surface layer (Skrzypek & Przybyłowicz, 2020). At a specific temperature and time, the near-surface zone is diffusely saturated with an element or elements in solid (Ucar et al., 2020; Xie et al., 2012), liquid (Ghelloudj et al., 2018; Kul et al., 2020; Sen et al., 2005), gaseous (Barnaby et al., 1975; Liu et al., 2020; Torchane, 2021) and plasma (Drajewicz et al., 2021) media. One such process is plasma nitriding, which aims to improve the anti-corrosive properties (Kusmič & Hrubý, 2015; Kusmič et al., 2021), fatigue resistance (Kovaci et al., 2016a) and abrasive wear (Karaoğlu, 2002; Kovaci et al., 2019) of steels, titanium alloys and iron matrix sinters (Çelik et al., 2000; Rakowski et al., 2006).



The plasma nitriding process is carried out under vacuum. After the charge is gradually heated to the required temperature by cathodic screens or resistance heating in the furnace retort, gas is delivered to the retort at a fixed pressure of $10^{-2} \div 1$ Pa. The nitrated elements are at negative potential with respect to the furnace walls, the anode is the furnace retort. The applied voltage induces a glow discharge. In an electric field, ionisation of the gas takes place, whose positive ions and high-energy neutral particles bombard the surfaces of the workpieces. This results in the release of heat necessary for the thermal activation of the nitrogen and its diffusion, as well as the occurrence of cathodic sputtering, which removes a layer of passive oxides from the surface. The surface of the objects is developed by making grain boundaries and other defects in the crystal structure visible. The described process favours the activation of the surface so that the adsorption and nucleation of new phases is facilitated, thus eliminating the problem of overcoming the surface passivity barrier. Nitrogen atoms form FeN nitrides with the precipitated iron atoms, which are adsorbed onto the surface of the product and then decompose. Iron and alloying element atoms combine with diffusing nitrogen atoms to form nitrides (Aghajani & Behranghi, 2017; Blicharski, 2012; Burakowski & Wierzchoń, 1995; Chattopadhyay, 2004; Dobrzański, 2006; Kula, 2000; Przybyłowicz, 1999; Świć & Gola, 2017).

The surface layers formed during the nitriding process are characterised by a zonal structure. They may include phases from the iron-nitride system such as γ' , ε and solid solution α (Głowacki et al. 2005a; Wang et al., 2013). The compound layer, otherwise known as the white zone, is formed by Fe_{2-3}N and Fe_4N nitrides, often also $\text{Fe}_2(\text{C}_x\text{N}_y)$ carbide nitrides. The dominant phase near the surface is the ε -phase, the content of which decreases moving deeper into the material, while the content of the γ' phase increases until it dominates in front of the diffusion zone (Głowacki et al., 2005b). It is not only the presence of the ε phase that is responsible for the porosity of the white zone, as demonstrated by (Michalski et al., 2005) during a controlled gas nitriding process. They observed that porosity is formed in layers of compounds consisting of ε and γ' phase as well as in layers with γ' phase only. The Fe_{2-3}N nitride layer is characterized by greater hardness and brittleness than the Fe_4N layer. It is also more resistant to wear and corrosion. The Fe_4N nitride layer tolerates overload more favorably and has a higher resistance to fracture. The values of the thermal expansion coefficients of the γ' and ε phases are different, making the compound layer prone to cracking and falling off at the interface (Spies & Dalke, 2014). Given the properties of the ε and γ' phases that make up the white zone, it is described as hard and resistant to abrasive and adhesive wear. It is also brittle, which, if thicker, can result in spalling in service (Lan & Wen, 2012; Yang et al., 2017). The compound layer is often removed from the component before use by grinding, polishing or chemical etching in solutions of cyan compounds (Czerwiński, 2012). The microstructure of the core matrix of the nitrated component coincides with the microstructure of the diffusion zone matrix. When the limiting solubility of nitrogen in the zone is exceeded, fine nitrides of the alloying elements aluminium, chromium, molybdenum, vanadium and tungsten are released. Their presence causes an increase in hardness by distorting the crystal structure of the matrix (Blicharski, 2012; Czerwiński, 2012; Wang & Chung, 2013). The diffusion zone is characterised by higher impact strength than the white zone (Zhang & Bell, 1985). It also determines the strength of the nitrated layer; due to its high resistance to thermal fatigue and abrasive wear (Lan & Wen, 2012; Yang et al., 2017). Furthermore, the resulting coating increases resistance to seizure, corrosion and the tempering effect of heat.

The main advantage of plasma nitriding is that it is possible to form a layer of compounds with only the ε or γ' phase, or to produce a nitrated layer consisting only of the diffusion zone. Plasma nitriding allows diffusion of nitrogen across grain boundaries and lattice diffusion (Blicharski, 2012). The advantage of this process is a surface with much less roughness than gas nitriding and minimal distortion of the feedstock. Therefore, products after the process do not require additional machining (Aghajani & Behranghi, 2017; Spies & Dalke, 2014).

In order to make the best use of the nitriding potential, special steels with a specific chemical composition have been developed containing, among others, aluminium, chromium, molybdenum and vanadium, which have a high affinity for nitrogen (Blicharski, 2012; Spies & Dalke, 2014). The carbon content should not exceed 0.5 % because chromium, molybdenum and vanadium form stable carbides, hindering the formation of nitrides (Aghajani & Behranghi, 2017). Due to the low solubility of nitrogen, the alloying elements separate almost entirely in the form of finely dispersed nitrides. The resulting volume difference causes local distortion of the crystal lattice, resulting in a strengthening effect and increased solubility of nitrogen in the iron matrix (Spies & Dalke, 2014). The presence of alloying additives in the surface layer increases hardness, provides high hardenability and resistance to temper-

ing embrittlement (Blicharski, 2017; Burzyńska-Szysko, 2011; Chattopadhyay, 2004). With increasing nitriding time and temperature, coagulation of the precipitated nitrides can occur, as indicated by a decrease in hardness. Under constant nitriding process conditions, an increase in the content of alloying additives results in a decrease in the depth of the compound layer. In the case of alloyed steels, an increase in the content of nitride-forming elements leads to a decrease in the thickness of the diffusion layer and an increase in hardness at its surface (Spies & Dalke, 2014). Also the process atmosphere influences the microstructure of the nitrided layers. A small addition of oxidising compounds to the nitriding mixture during plasma or gas nitriding has a beneficial effect on the nitrided layer - the presence of oxygen stabilises the ϵ -phase and increases the growth rate of the layer (Czerwiński, 2012).

Appropriate selection of the process parameters makes it possible to obtain surface layers with a variety of structures, which is much more difficult in the case of conventional nitriding methods (Çelik et al., 2000; Karaoğlu, 2003; Rakowski et al., 2006). An analysis of the literature (Albarran et al., 1992; Berkowski, 2005; Blicharski, 2012; Borgolli et al., 2002; Głowacki et al., 2005a, 2005b; Höck et al., 1996; Karamiş et al., 2019; Kovaci et al., 2016b; Krbařa et al., 2019; Kusmič et al., 2021; Ozbaysal et al., 1986; Podgornik & Vižintin, 1999, 2001; Skonieski et al., 2013; Zhao et al., 2021) allows us to conclude that it is preferable to produce nitrided layers consisting of a compound zone and a diffusion zone. However, for some applications, a more favourable set of properties is offered by the diffusion layer alone - good resistance to abrasive wear, thermal fatigue and impact strength. Hot working dies are subjected to harsh working conditions such as repeated impacts and heating and cooling cycles. Plasma nitriding of hot work dies made from AISI H13 steel allowed only a diffusion zone to be obtained, resulting in a 10-fold increase in the service life of the machined tools (Peng et al., 2020). In order to create a nitrided layer with only a diffusion layer, it is necessary to limit the nitrogen content of the nitriding mixture.

Literature data (Blicharski, 2012) indicate the following chemical composition of the nitriding gas mixture: 1-5% nitrogen, the rest carrier gas. Podgornik and Vižintin (1999), wishing to form a nitrided layer without a compound zone on 42CrMo4 heat-treatable steel, proposed the following parameters for the plasma nitriding process: gas mixture composition 0.6% N₂ and 99.4% H₂, temperature 540°C and time 17 h. When observing the microstructure, a forming layer of compounds was noticed in addition to the diffusion layer. In the work (Skonieski et al., 2013), the tempering steel 42CrMo4 was subjected to plasma nitriding. The process took place at 500°C and the variables were time and composition of the gas mixture. No white zone was observed during microscopic examination although the results of the analysis of the glow discharge optical emission spectroscopy (GDOES) profiles suggested its presence (depths of less than 1 µm). Kovaci et al. (2016a), for 42CrMo4 steel, obtained a white zone depth of 1-2 µm and a diffusion zone of 120-130 µm, during the process at 400°C with a gas mixture of 50% N₂ and 50% H₂. Głowacki et al. (2005a) investigated the effect of the nitrogen content of the H₂-N₂ mixture on the plasma nitriding process of 38HMJ nitridable steel and WCL hot work tool steel. The treatment was carried out for 2 h at 550°C. From the diffractograms, it was found that the structure of the layers formed on 38HMJ and WCL steels consisted of: solution α - at 3% N₂, solution α and phase γ' - at 5% N₂, solution α , phase γ' and ϵ - at 9% N₂ and solution α and phase γ' at 26% N₂. A thin layer of iron nitrides (9% N₂) and a solid film of iron nitrides and alloying additives (26% N₂) were also observed. In (Da Silva Rocha et al., 1999), AISI M₂ tool steel was plasma nitrided at 350, 400, 450 and 500°C with a gas mixture of 5% N₂ and 95% H₂ for 30 min. A nitrided layer consisting of a diffusion zone alone was obtained, the depth of which increased with increasing nitriding time.

The aim of this study was to determine the influence of the plasma nitriding process parameters and the chemical composition of the substrate material on the microstructure of the nitride layers formed, on the substrates of selected tool steels, and to determine the growth kinetics of the diffusion layer below. The influence of chemical composition of tool steels from each group (cold work, hot work and HSS) on nitriding process was investigated. The plasma nitriding time was selected as a main factor of coatings formation. The all processes were conducted in semi-industrial conditions.

2. Experimental

According to experimental plan plasma nitriding, at 550°C and times of 2, 4 and 6 hours, was carried out on five selected tool steels, the chemical composition of which is shown in Table 1. Process was conducted using industrial system (Ionit, Sulzer-Metaplas, Germany).

Table 1. Chemical composition of steel according to EN ISO 4957 (2004) and PN-H-85023 (1986) standards.

Steel designation	Chemical composition [wt.%]								
	C	Si	Mn	P	S	Cr	Mo	V	W
60WCrV8	0.55-0.65	0.70-1.00	0.15-0.45	-	-	0.90-1.20	-	0.10-0.20	1.70-2.20
90MnCrV8	0.85-0.95	0.10-0.40	1.80-2.20	-	-	0.20-0.50	-	0.05-0.20	-
145Cr6	1.30-1.45	0.15-0.40	0.40-0.70	≤0.030	≤0.030	1.30-1.65	-	0.10-0.25	-
X37CrMoV5-1	0.33-0.41	0.80-1.20	0.25-0.50	-	-	4.80-5.50	1.10-1.50	0.30-0.50	-
HS6-5-2	0.80-0.88	≤0.45	-	-	-	3.80-4.50	4.70-5.20	1.70-2.10	5.90-6.70

The samples, measuring $\text{Ø}30 \text{ mm} \times 30 \text{ mm}$, were supplied in tempered condition from one batch of steels. The surfaces to be tested were sandblasted with electrocorundum and then ground on an ATM GmbH Saphir 330 grinder with SiC grit sandpaper with a gradation of 80 to 500. 90 specimens were prepared - 2 specimens for each steel grade at three time variants: 2 h, 4 h and 6 h. The time variants were chosen for optimisation of nitriding time and selection of shortest time for diffusion layer formation. Before the processes, the samples were cleaned in an ultrasonic cleaner. The invariant process parameters are shown in Table 2. The process was controlled and monitored using built-in software in nitriding system. The composition of plasma gasses was selected for formation only of diffusion layer without outer nitride layers.

Table 2. Plasma nitriding process parameters.

Composition of nitrated mixture, l/h	Temperature, °C	Frequency, kHz	Voltage, V	Intensity, A	Pressure, mbar	Pulse
5N ₂ + 95H ₂	550	10	400	15	3.6	20/80

After the plasma nitriding processes, metallographic samples were taken. The microstructure of the nitrated layers was studied on a Phenom XL scanning electron microscope from PIK Instruments, using a back-scattered electron detector - BSE. The coating thickness was measured in 10 places on the cross-section of sample and average thickness value was calculated. The chemical composition was analysed using a secondary X-ray energy dispersive spectrometer - EDS, integrated with the Phenom XL microscope. Maps showing the relative content of chemical elements from the analysed areas were obtained. All samples were etched with Nital 4% to measure the depth of the layers formed. The phase composition was analysed using X-ray diffraction (XRD) method and ARL X'TRa diffractometer.

3. Results and discussion

3.1. Cold-work tool steel 60WCrV8

The microstructure of the 60WCrV8 steel, after each of the three nitriding processes (Fig. 1a-c), consists of a dark matrix and bright irregularly shaped precipitates, occurring mainly on the grain boundaries. The increased concentration of tungsten in the chemical composition analysis maps (Fig. 1) indicates that these are tungsten carbides. This is also indicated by the carbon content (0.55-0.65 wt.%), which may have increased the ability of the alloying additives to form carbides and decreased the ability to form nitrides (Aghajani & Behrangi, 2017). The near-surface layers of 60WCrV8 steel after plasma nitriding at 2, 4 and 6 h show areas of increased nitrogen concentration, the amount of which decreases with increasing distance from the surface of the samples. During the plasma nitriding process at 2 h, a diffusion layer with an average depth of 0.79 μm , was obtained. After 4 h of the process, a layer with an average depth of 2.14 μm was obtained, and after 6 h: 2.12 μm . The XRD phase analysis from the surface of sample showed presence of Fe₄N (γ') and Fe₃N (ϵ) nitrides (Fig. 2). It confirms the formation of thin nitrides layer on the surface of samples. The presence of FeO oxides was also confirmed by XRD phase analysis.

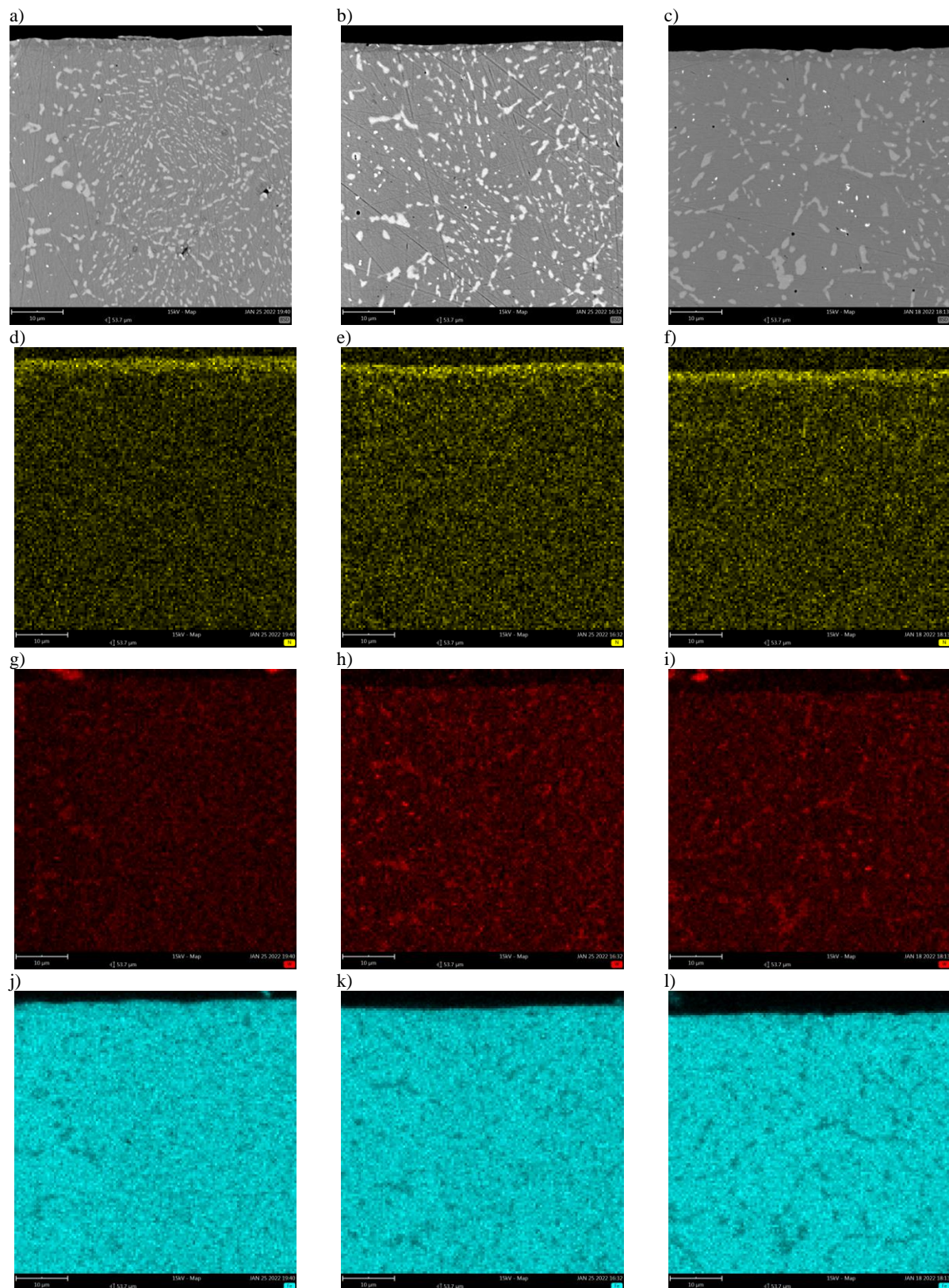


Fig. 1. a)-l) Microstructure of the layer after 2, 4 and 6 h of the nitriding process carried out on a tool steel grade 60WCrV8 substrate and the result of the relative concentrations of nitrogen, tungsten and iron.

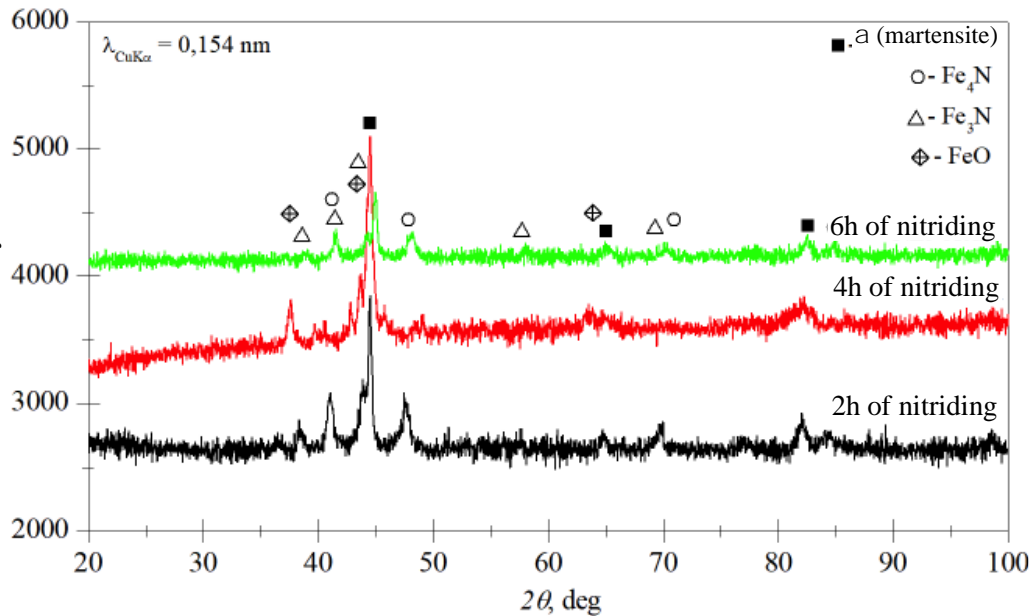


Fig. 2. The results of XRD phase analysis from samples of 60WCrV8 cold work steel after 2, 4 and 6h of plasma nitriding process.

3.2. Cold-work tool steel 90MnCrV8

The results of XRD phase analysis confirmed the formation of Fe_4N (γ') nitride as well as FeO on the surface of 90MnCrV8 steel samples after plasma nitriding process (Fig. 3). The microstructure of samples after plasma nitriding at 2, 4 and 6 h (Fig. 4a-c) consists of a light matrix and dark globular precipitates. They are uniformly distributed in the microstructure, mainly in the grains, but also at the grain boundaries (Fig. 4a-c). Identification of the precipitates requires further study. The near-surface layer of the samples shows areas of slightly increased nitrogen concentration, the amount of which decreases with increasing distance from the surface of the samples (Fig. 4d-f). This indicates the formation of a diffusion layer on the substrate of the 90MnCrV8 steel, plasma nitrided at 2, 4 and 6 h. No nitrides were observed in the microstructure of the steel, as confirmed by the chemical composition analysis. No changes in iron and chromium concentrations were observed (Fig. 4g-l). The high carbon content (0.85-0.95 wt.%) and the low content of nitride-forming elements (0.20-0.50 wt.% chromium and 0.05-0.20 wt.% vanadium) hinder the possibility of alloy additive nitride formation (Aghajani & Behrangi, 2017; Blicharski, 2012). The average layer depth is 1.17 μm , for treatment after 2 h. After the nitriding process at 4 h, the average layer depth is 0.66 μm , and after 6 h: 0.57 μm .

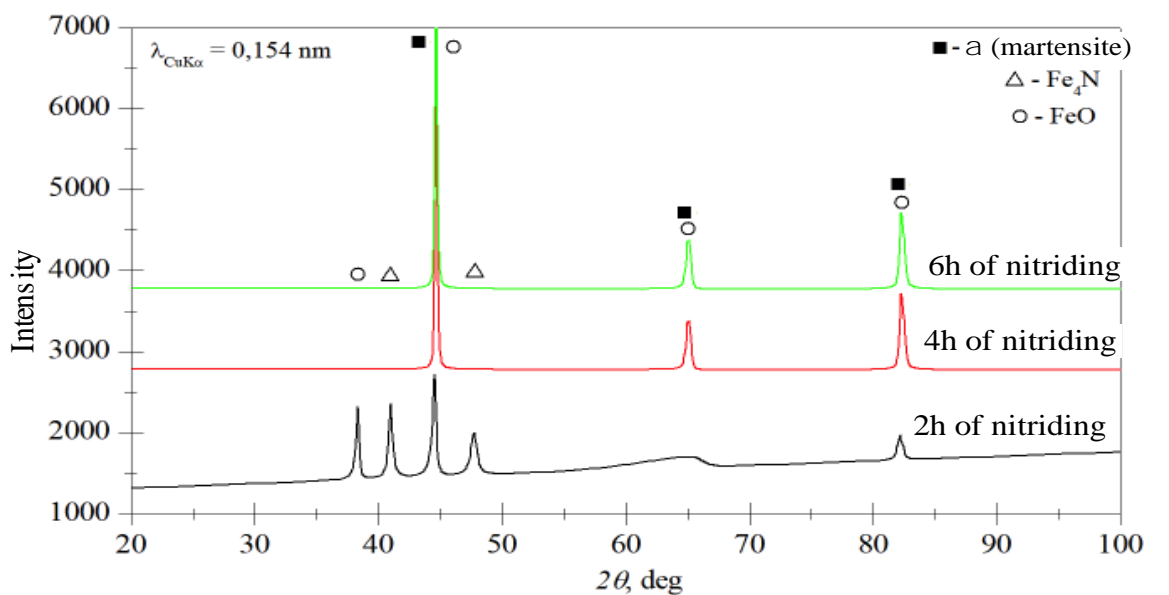


Fig. 3. The results of XRD phase analysis from samples of 60WCrV8 cold work steel after 2, 4 and 6h of plasma nitriding process.

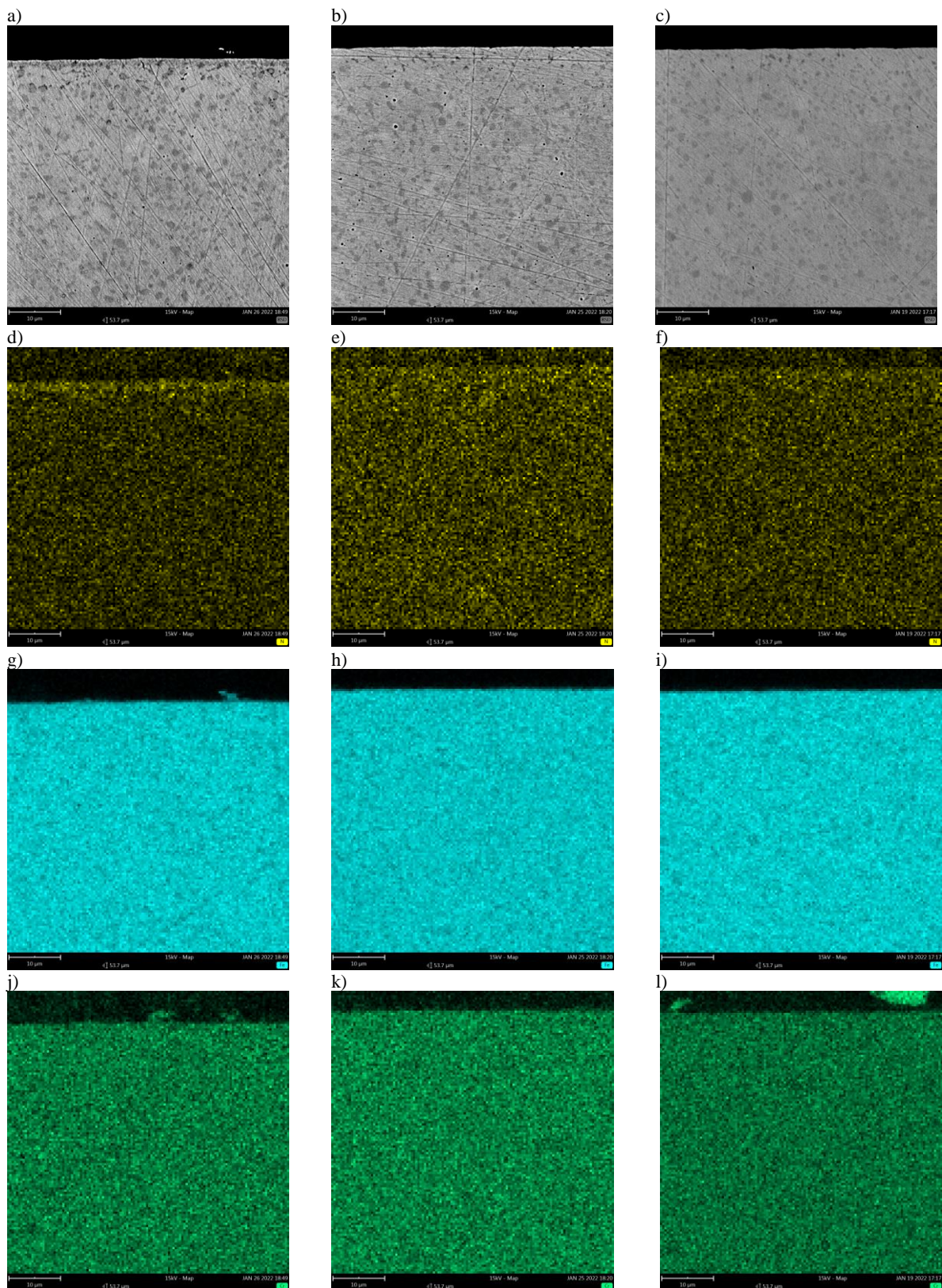


Fig. 4. a-l) Microstructure of the layer after 2, 4 and 6 h of the nitriding process carried out on a tool steel grade 90MnCrV8 substrate and the result of the relative concentrations of nitrogen, iron and chromium.

3.3. Cold-work tool steel 145Cr6

The XRD phase analysis showed the presence of F_4N (γ') phase on the surface of 145Cr6 samples after each plasma nitriding process conditions (Fig. 5). The microstructure of 145Cr6 steel, after each of the three plasma nitriding processes (Fig. 6a-c), consists of a light matrix and irregularly shaped

dark precipitates arranged in bands perpendicular to the surface. Plasma nitriding of 145Cr6 steel for 2 h leads to the formation of a diffusion layer, as evidenced by the increased nitrogen intensity near the surface (Fig. 6d). The layer formed is porous (Fig. 6a). Its depth is approximately 1.65 μm . The change in iron and chromium content is negligible, as evidenced by the surface analysis of these elements shown in Fig. 6g, j. The result of plasma nitriding for 4 h is a diffusion layer with an average depth of 11.72 μm , as confirmed by the chemical composition analysis performed (Fig. 6e). The nitrogen content decreases from the surface into the depth of the material. In Fig. 6b, no dark precipitates are observed in the diffusion layer, the presence of which was identified in the layers formed during the plasma nitriding process at 2 and 6 h. A small number of pores are also visible. Plasma nitriding of 145Cr6 steel at 6 h leads to the formation of a nitrided layer consisting of a white zone and a diffusion zone, as evidenced by the increased nitrogen intensity near the surface, which decreases deep into the substrate (Fig. 6c,f). The resulting white layer is neither continuous nor adherent, as can be seen in Fig. 6c. In the region of about 10 μm from the white layer-diffusion layer boundary, large longitudinal and globular-shaped separations are no longer visible. The average depth of the white layer is 1.50 μm , while that of the entire nitrided layer is 14.32 μm .

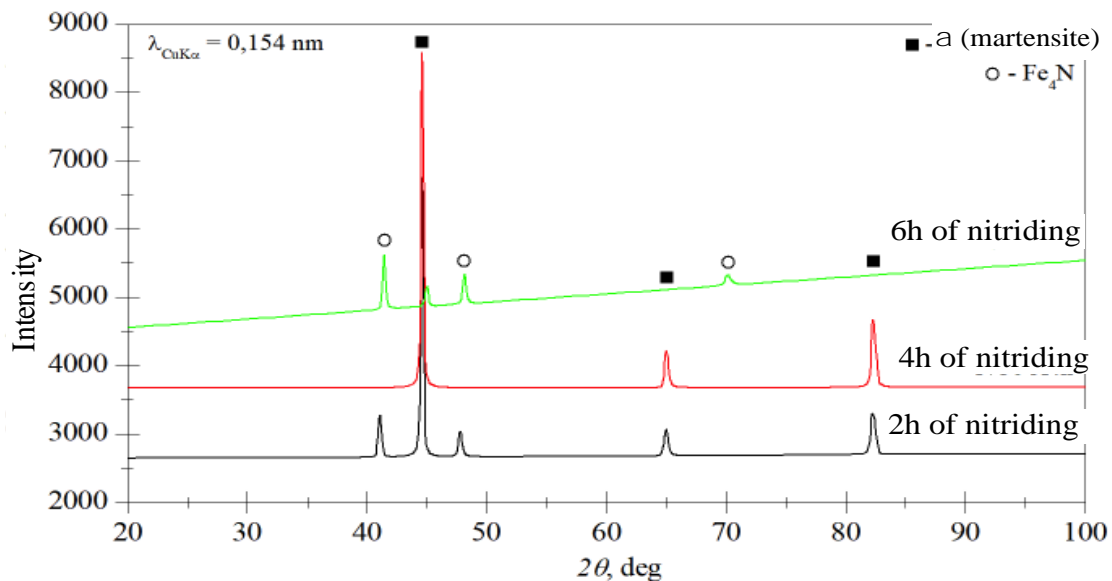


Fig. 5. The results of XRD phase analysis from samples of 145Cr6 cold work steel after 2, 4 and 6h of plasma nitriding process.

4. Summary

On the basis of microstructure photographs, relative elemental concentration analysis, it was shown that plasma nitriding of selected tool steels, carried out for 2, 4 and 6 h, in a nitriding mixture of 5% N₂ and 95% H₂ and at 550°C, leads for most of the analysed steels to the formation of diffusion/nitrided layers on their substrate. The time of the plasma nitriding process has an ambiguous effect on the depth of the nitrided layers formed on the substrate of the selected steels. The parabolic-like growth pattern of the nitrided layer was found to be characteristic of steels with high alloying element content: HS6-5-2.

The formation of a diffusion layer was observed on the substrate of each steel flux-nitrided in a mixture consisting of 5% N₂ and 95% H₂. The formation of a white layer was also observed during the nitriding of 145Cr6 steel at 6 h. Chromium nitrides were formed in the diffusion layer of the hot-work steel X37CrMoV5-1. In high-speed steel HS6-5-2, no nitrides were observed despite the high content of nitride-forming additives. Literature data (Doan et al., 2016) report that for high-speed steels, vanadium-rich primary MC carbides are converted to nitrides very slowly. Inside these types of carbides and nitrides, the diffusion coefficient of nitrogen is very low. According to Lachtin and Kogan (1982), the diffusion coefficient of vanadium nitride at 550°C is 1016 lower compared to ferrite. The formation of very thin layers and the absence of nitrides in the 60WCr5 and 90MnCrV8 steels is attributed to the low content of nitride-forming elements (Table 1). Literature data indicate that the reduction in the possibility of nitride formation is also influenced by the higher carbon content (compared to nitridable steels - above 0.4 wt.%).

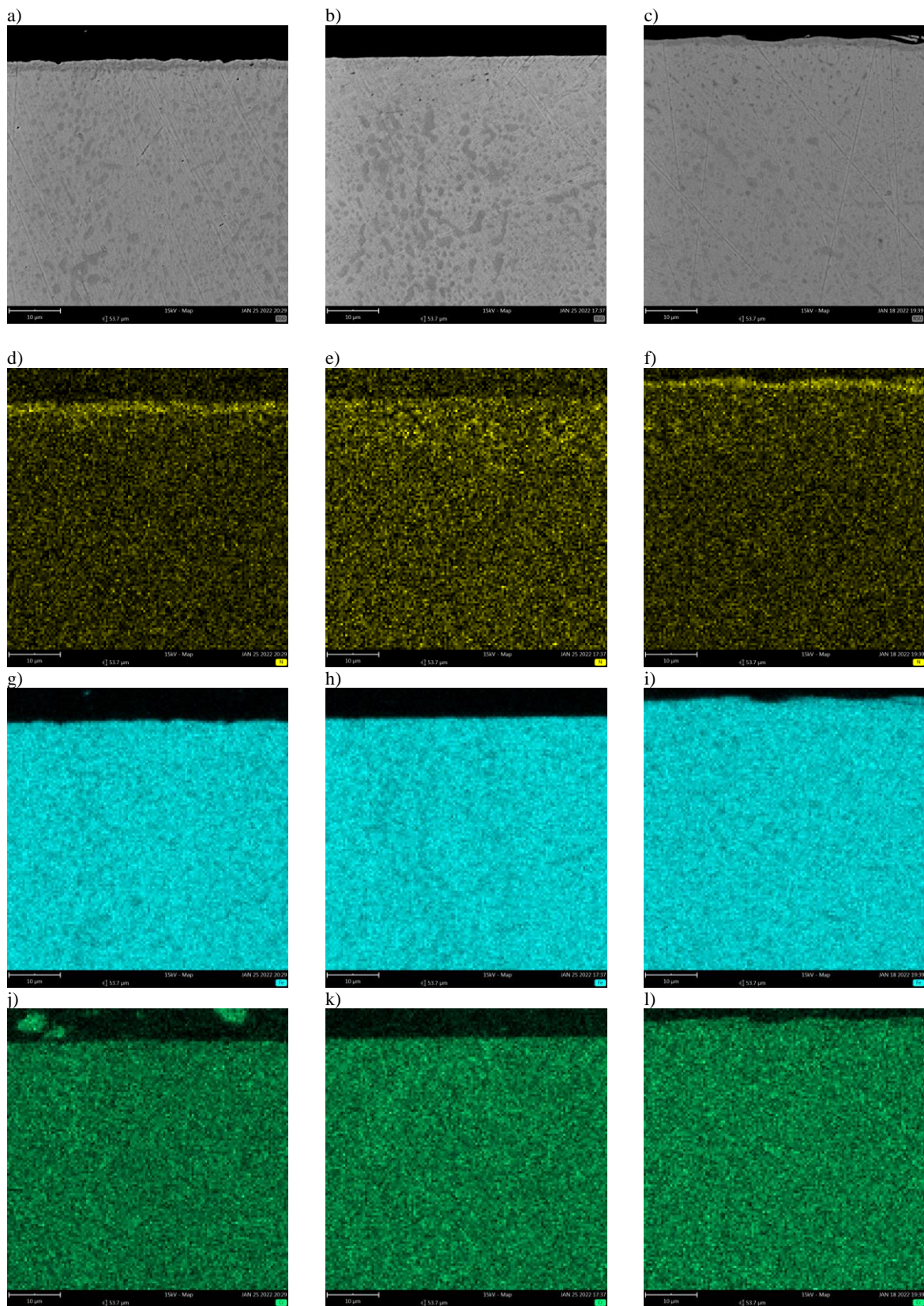


Fig. 6. a)-l) Microstructure of the layer after 2, 4 and 6 h of the nitriding process carried out on a substrate of 145Cr6 tool steel and results of the analysis of the relative concentrations of nitrogen, iron and chromium.

5. Conclusions

- 1) The presence and morphology of the resulting nitrided layer, formed on the substrate of 60WCr5, 90MnCrV8, 145Cr6, X37CrMoV5-1 and HS6-5-2 steels, during plasma nitriding at

550°C in a mixture of 5% N₂ and 95% H₂, depends on the duration of the process and the chemical composition of the nitrided steel.

- 2) An increase in the duration of plasma nitriding, results in an increase in the depth of the nitrided layer formed on the substrate of high-alloy steels X37CrMoV5-1 and HS6-5-2.
- 3) Nitriding in a mixture of 5% nitrogen and 95% hydrogen produces a nitrided layer without a compound zone.
- 4) The presence and mass content of nitride-forming elements influences the formation of alloying additive nitrides in the microstructure of the diffusion layer.
- 5) Nitrides of alloying additives, present in the diffusion layer, are formed in the hot-work steel X37CrMoV5-1.
- 6) The results obtained indicate that X37CrMoV5-1 steel due to their alloying element content and carbon content - are the most suitable for the plasma nitriding process among the analysed steels.

Acknowledgement

The research was financially supported by National Research and Development Centre under grant no. TECHMATSTRATEG-III/0002/2019.

References

- Aghajani, H., & Behrangi, S. (2017). *Plasma nitriding of steels*. Springer International Publishing.
- Albarran, J. L., Juárez-Islas, J. A., & Martinez, L. (1992). Nitride width and microstructure in H-12 ion nitrided steel. *Materials Letters*, 15, 68-72.
- Barnaby, J. T.; Haq, M. I., & Smith, C. G. (1975). Toughness of carburized steels. *Metals Technology*, 2(1), 535-537. <https://doi.org/10.1179/030716975803276871>
- Berkowski, L. (2005). Wpływ struktury na skutki azotowania chromowych stali ledeburytycznych. Część 1: Informacje o materiale do badań. *Obróbka Plastyczna*, 5, 5-15.
- Blicharski, M. (2012). *Inżynieria powierzchni*. Wydawnictwa Naukowo-Techniczne.
- Blicharski, M. (2017). *Inżynieria materiałowa stali*. Wydawnictwo Naukowe PWN.
- Borgoili, F., Galvanetto, E., Fossati, A., & Bacci, T. (2002). Glow-discharge nitriding and post-oxidising treatments of AISI H11. *Surface and Coatings Technology*, 162(1), 61-66. [https://doi.org/10.1016/S0257-8972\(02\)00574-1](https://doi.org/10.1016/S0257-8972(02)00574-1)
- Burakowski, T., & Wierzchoń, T. (1995). *Inżynieria powierzchni metali*. Wydawnictwa Naukowo-Techniczne.
- Burzyńska-Szysko, M. (2011). *Materiały konstrukcyjne*. Politechnika Warszawska.
- Chattopadhyay, R. (2004). *Advanced thermally assisted surface engineering process*. Springer. <https://doi.org/10.1007/b105271>
- Czerwinski, F. (2012). *Thermochemical treatment of metals. heat treatment – conventional and novel applications*. IntechOpen.
- Çelik, A., Efeoğlu, I., & Sakar, G. (2000). Microstructure and structural behavior of ion-nitrided AISI 8620 steel. *Materials Characterization*, 46(1), 39-44. [https://doi.org/10.1016/S1044-5803\(00\)00091-7](https://doi.org/10.1016/S1044-5803(00)00091-7)
- da Silva Rocha, A, Strohaecker, T., Tomala, V., & Hirsch, T. (1999). Microstructure and residual stresses of plasma-nitrided M2 tool steel. *Surface Coatings Technology*, 115 (1), 24-31. [https://doi.org/10.1016/S0257-8972\(99\)00063-8](https://doi.org/10.1016/S0257-8972(99)00063-8)
- Doan, T. V., Dobrocký, D., Pokorný, Z., Kusmic, D., & Nguyen, V. T. (2016). Effect of plasma nitriding on mechanical and tribological properties of 42CrMo4. *ECS Transactions*, 74(1), 231-238. <https://doi.org/10.1149/07401.0231ecst>
- Dobrzański, L. A. (2006). *Podstawy nauki o materiałach i metaloznawstwo. Materiały inżynierskie i projektowanie materiałowe*. Wydawnictwa Naukowo-Techniczne.
- Drajewicz, M., Góral, M., Pytel, M., Kościelniak, B., Kubaszek, T., Wierzba, P., & Cichosz, P. (2021). The duplex coating formation using plasma nitriding and CrN PVD deposition on X39CrMo17-1 stainless steel. *Solid State Phenomena* 320, 43-48. <https://doi.org/10.4028/www.scientific.net/SSP.320.43>
- EN ISO 4957. (2004). European Committee for Standardization. Stale narzędziowe.
- Ghelloudj, E., Hannachi, M. T., & Djebaili, H. (2018). Effect of time of the compound layer formed during salt bath nitriding of AISI 4140 steel. *Acta Metallurgica Slovaca* 24(4), 280-286. <https://doi.org/10.12776/ams.v24i4.1111>
- Głowacki, S., Majchrzak, A., & Majchrzak, W. (2005a). Wpływ proporcji składników atmosfery azotującej na strukturę warstwy azotowanej jonowo. *Obróbka Plastyczna Metali*, 2, 15-22.

- Głowacki, S., Majchrzak, A., & Majchrzak, W. (2005b). Zależność grubości warstwy azotowanej jonowo od proporcji składników atmosfery azotującej. *Obróbka Plastyczna*, 1, 37-46.
- Höck, K., Soies, H-J., Larisch, B., Leonhardt, G., Buecken, B. (1996). Wear resistance of prenitrided hardcoated steels for tools and machine components. *Surface and Coatings Technology*, 88(1-3), 44-49. [https://doi.org/10.1016/S0257-8972\(96\)02914-3](https://doi.org/10.1016/S0257-8972(96)02914-3)
- Karamiş, M. B., Yıldızlı, K., & Aydın, G. C. (2019). Sliding/rolling wear performance of plasma nitrided H11 hot working steel. *Tribology International*, 51, 18-24. <https://doi.org/10.1016/j.triboint.2012.02.005>
- Karaoğlu, S. (2002). Structural characterization and wear behaviour of plasma-nitrided AISI 5140 low-alloy steel. *Materials Characterization*, 49(4), 349-357. [https://doi.org/10.1016/S1044-5803\(03\)00031-7](https://doi.org/10.1016/S1044-5803(03)00031-7)
- Kovacı, H., Hacısalihoğlu, İ., Yetim, A. F., & Çelik, A. (2019). Effects of shot peening pre-treatment and plasma nitriding parameters on the structural, mechanical and tribological properties of AISI 4140 low-alloy steel. *Surface & Coatings Technology*, 358, 256-265. <https://doi.org/10.1016/j.surfcoat.2018.11.043>
- Kovacı, H., Yetim, A. F., Baran, O., & Celik, A. (2016a). Fatigue crack growth analysis of plasma nitrided AISI 4140 low-alloy steel: Part 1-constant amplitude loading. *Materials Science & Engineering: A*, 627, 257-264. <https://doi.org/10.1016/j.msea.2016.07.002>
- Kovacı, H., Yetim, A. F., Baran, Ö., & Çelik, A. (2016b). Fatigue crack growth analysis of plasma nitrided AISI 4140 low-alloy steel: Part 2-Variable amplitude loading and load interactions. *Materials Science & Engineering: A*, 627, 265-275. <https://doi.org/10.1016/j.msea.2016.07.003>
- Krbaťa, M., Majerik, J., Barényi, I., Mikušová, I., & Kusmič D. (2019). Mechanical and tribological features of the 90MnCrV8 steel after plasma nitriding. *Manufacturing Technology*, 19(2), 238-242. <https://doi.org/10.21062/ujep/276.2019/a/1213-2489/MT/19/2/238>
- Kul, M., Danacai, I., Gezer, Ş., & Kacara, B. (2020). Effect of boronizing composition on hardness of boronized AISI 1045 steel. *Materials Letters*, 279, Article 128510. <https://doi.org/10.1016/j.matlet.2020.128510>
- Kula, P. (2000). *Inżynieria warstwy wierzchniej*. Wydawnictwo Politechniki Łódzkiej.
- Kusmič, D., & Hrubý, V. (2015). Corrosion resistance of plasma nitrided structural steels. *Manufacturing Technology*, 15(1), 64-69. <http://dx.doi.org/10.21062/ujep/x.2015/a/1213-2489/MT/15/1/64>
- Kusmič, D., Čech, O., & Klakurková, L. (2021). Corrosion resistance of ferritic stainless steel X12Cr13 after application of low-temperature and high-temperature plasma nitriding. *Manufacturing Technology*, 21(1), 98-104. <https://doi.org/10.21062/mft.2021.013>
- Lachin, J. M., & Kogan, J. D. (1982). *Structure and strength of nitrided alloys*. Metallurgia.
- Lan, H-Y., & Wen, D-C. (2012). Improving the erosion and erosion-corrosion properties of precipitation hardening mold steel by plasma nitriding. *Materials Transactions*, 53(8), 1443-1448. <https://doi.org/10.2320/matertrans.M2012083>
- Liu, Z., Peng, Y., Chen, C., Gong, J., & Jiang, Y. (2020). Effect of surface nanocrystallization on low temperature gas carburization for AISI 316L austenitic stainless steel. *International Journal of Pressure Vessels and Piping*, 182, Article 104053. <https://doi.org/10.1016/j.ijpvp.2020.104053>
- Luty, W. (1977). *Poradnik inżyniera. Obróbka cieplna stopów żelaza*. Wydawnictwo Naukowo-Techniczne.
- Michalski, J., Tacikowski, J., Wach, P., Lunarska, E., & Baum, H. (2005). Formation of single-phase layer of γ' -nitride in controlled gas nitriding. *Metal Science and Heat Treatment*, 47(11), 516-519. <https://doi.org/10.1007/s11041-006-0023-0>
- Ozbaysal, K., Inal, O. T., & Romig Jr., A. D. (1986). Ion-nitriding behavior of several tool steels. *Materials Science & Engineering*, 78 (2), 179-191. [https://doi.org/10.1016/0025-5416\(86\)90322-8](https://doi.org/10.1016/0025-5416(86)90322-8)
- Peng, T., Zhao, X., Chen, Y., Tang, L., Wei K. & Hu, J. (2020). Improvement of stamping performance of H13 steel by compound-layer free plasma nitriding. *Surface Engineering*, 36(5), 492-497. <https://doi.org/10.1080/02670844.2019.1609172>
- Pessin, M.A., Tier, M.D., Strohaecker, T.R., Bloyce, A., Sun, Y., & Bell, T. (2000). The effects of plasma nitriding process parameters on the wear characteristics of AISI M2 tool steel. *Tribology Letters*, 8, 223-228. <https://doi.org/10.1023/A:1019199604963>
- PN-H-85023. (1986). Polski Komitet Normalizacyjny. Stal narzędziowa stopowa do pracy na zimno – Gatunki.
- Podgornik, B., & Vižintin, J. (1999). Wear properties of plasma nitrided steel in dry sliding conditions. *Journal of Tribology*, 121(4), 802-807. <https://doi.org/10.1115/1.2834138>
- Podgornik, B., & Vižintin, J. (2001). Wear resistance of pulse plasma nitrided AISI 4140 and A355 steels. *Materials Science and Engineering: A*, 315(1-2), 28-34. [https://doi.org/10.1016/S0921-5093\(01\)01202-3](https://doi.org/10.1016/S0921-5093(01)01202-3)
- Przybyłowicz, K. (1999). *Metaloznawstwo*. Wydawnictwa Naukowo-Techniczne.
- Rakowski, W. A., Kot, M., Zimowski, S., & Wierchoń, T. (2006). Właściwości warstw azotowanych jarzenio-wo, wytworzonych na stali 316L. *Problemy Eksploatacji*, 3, 107-116.

- Sen, S., Sen, U., & Bindal, C. (2005). The growth kinetics of borides formed on boronized AISI 4140 steel. *Vacuum*, 77(2), 195-202. <https://doi.org/10.1016/j.vacuum.2004.09.005>
- Skonieski, A. F. O., dos Santos, G. R., Hirsch, T. K., & da Silva Rocha, A. (2013). Metallurgical response of an AISI 4140 steel to different plasma nitriding gas mixtures. *Materials Research*, 16(4), 884-890. <https://doi.org/10.1590/S1516-14392013005000073>
- Skrzypek, S. J., Przybyłowicz, K. (2020). *Inżynieria metali i technologie materiałowe*. Wydawnictwo Naukowe PWN.
- Spies, H.-J., Dalke, A. (2014). Case structure and properties of nitrided steel. *Comprehensive Materials Processing*, 12, 438-488. <https://doi.org/10.1016/B978-0-08-096532-1.01216-4>
- Staub, F., Haas, J., Malkiewicz, T., Orzechowski, S., Przegaliński, S. (1964). *Stal. Atlas metalograficzny struktur*. Wydawnictwa Naukowo-Techniczne.
- Świć, A., & Gola, A. (2017). *Współczesne technologie w inżynierii produkcji*. Politechnika Lubelska.
- Torchane, L. (2021). Influence of rare earths on the gas nitriding kinetics of 32CrMoNiV5 steel at low temperature. *Surfaces and Interfaces*, 23, 101016. <https://doi.org/10.1016/j.surfin.2021.101016>
- Ucar, N., Yigit, M., & Calik, A. (2020). Metallurgical characterization and kinetics of borodized 34CrNiMo6 steel. *Advanced in Materials Science*, 20(4(66)), 38-48. <https://doi.org/10.2478/adms-2020-0021>
- Wang, Q. J., & Chung, Y.-W. (2013). *Encyclopedia of tribology*. Springer <https://doi.org/10.1007/978-0-387-92897-5>
- Xie, F., Sun, L., & Pan, J. (2012). Characteristics and mechanisms of accelerating pack boriding by direct current field at low and moderate temperatures. *Surface & Coatings Technology*, 206(11-12), 2839-2844. <https://doi.org/10.1016/j.surfcoat.2011.12.003>
- Yang, R., Wu, G. L., Zhang, X., Fu, W. T., & Huang, X. (2017). Gradient microstructure and microhardness in nitrided 18CrNiMo7-6 gear steel. *IOP Conference Series: Materials Science & Engineering*, 219(1), 012047. <https://doi.org/10.1088/1757-899X/219/1/012047>
- Zhang, Z. L., & Bell, T. (1985). Structure and corrosion resistance of plasma nitrided stainless steel. *Surface Engineering*, 1(2), 131-136. <https://doi.org/10.1179/sur.1985.1.2.131>
- Zhao, F. S., Zhang, Z. H., Shao, M. H., Bi, Y. J., Wang, Z. W., Li, Y., Li, H. H., Xu, X. G., He, Y. Y. (2021). Mechanical and wear properties of 42CrMo Steel by plasma nitriding assisted hollow cathode ion source. *Materials Research*, 24(4), 1-10. <https://doi.org/10.1590/1980-5373-MR-2021-0137>

Wpływ Warunków Azotowania Plazmowego na Mikrostrukturę Powłok Uzyskanych na Podłożu Wybranych Stali Narzędziowych

Streszczenie

W pracy przedstawiono wyniki badań wpływu czasu procesu azotowania plazmowego na mikrostrukturę otrzymanych powłok. Jako materiał podłoża wybrano stale narzędziowe do pracy na zimno (60WCrV8, 90MnCrV8, 145Cr6), stale narzędziowe do pracy na gorąco (X37CrMoV5-1) oraz szybko tnące (HS6-5-2). Procesy prowadzono w warunkach przemysłowych z wykorzystaniem urządzenia Ionit firmy Oerlikon Metaplas ze zmiennymi czasami procesu 2, 4 i 6 godzin. Zgodnie z danymi literaturowymi wybrano mieszaninę azotującą składającą się z 5% azotu i 95% wodoru, co pozwoliło na uzyskanie oczekiwanej warstwy dyfuzyjnej bez warstwy białej (złożonej z azotków żelaza). Analiza mapowania pierwiastkowego wskazuje, że obecność i zawartość pierwiastków azototwórczych wpływa na powstawanie azotków dodatku stopowego w mikrostrukturze warstwy dyfuzyjnej. Stwierdzono również, że wydłużenie czasu azotowania plazmowego powoduje zwiększenie głębokości warstw azotowanych powstających na podłożu ze stali wysokostopowych: X37CrMoV5-1 i HS6-5-2. Azotki dodatków stopowych, obecne w warstwie dyfuzyjnej, powstają w wysokostopowej stali do pracy na gorąco X37CrMoV5-1, co wskazuje, że stale te są najbardziej odpowiednie do azotowania plazmowego spośród wszystkich analizowanych stali narzędziowych.

Słowa kluczowe: azotowanie plazmowe, stal narzędziowa, obróbka cieplna, kinetyka azotowania
